*Synthetic Metals*, 59 (1993) 253–258



## Short Communication

# Phase transitions and incommensurate states in GIC $C_{5n}HNO_3$*

A. M. Ziatdinov, N. M. Mishchenko and Yu. M. Nikolenko

*Institute of Chemistry, Far-East Branch of the Russian Academy of Sciences, Vladivostok 690022 (Russian Federation)*

(Accepted February 18, 1993)

## Abstract

ESR data of graphite intercalation compounds $C_{5n}HNO_3$ ($n=2$, 4) point at change of quantity and mobility of spin carriers in compounds of different stages and at intercalate crystallization ($T<250$ K). Crystallization (melting) of intercalate in second (fourth) stage compounds is a multistep (two-step) process with a 'global' temperature hysteresis. Reversible temperature variations of lineshapes of core C(1s), N(1s) and O(1s) X-ray photoelectrons at phase transitions can be explained assuming formation of charge density waves (CDWs) in surface layers of this compound.

## Introduction

The intercalation of ions and molecules into graphite leads both to anomalous changes in graphite properties and to rise of new properties: superconductivity, two-dimensional magnetism, structural incommensurability, etc. [1]. Particularly, in graphite intercalation compounds (GICs) with nitric acid, $C_{5n}HNO_3$ ($n=1, 2, \ldots$), two-dimensional liquid-like layers of $HNO_3$ of lower $T_c \simeq 250$ K are ordered and form a quasi-two-dimensional crystal which, particularly for $n=2$, is incommensurable with a carbon net along one of its crystallographic directions [2–4]. Therefore, $C_{5n}HNO_3$ compounds draw special attention as objects suitable for study of various problems of physics and chemistry of low-dimensional systems, especially of quasi-two-dimensional crystallization (melting) in periodic external potential and its dependence on stage index.

The present paper gives an account of the results of ESR studies in GIC $C_{5n}HNO_3$ ($n=2$, 4), unknown peculiarities of parameter variations of lineshapes of conduction electrons and electron spectroscopy for chemical analysis (ESCA) studies of the changes in electronic structure of the surface

*Originally submitted to ICSM '92, Göteborg, Sweden, August 1992.

0379-6779/93/$6.00

layers at intercalate 'freezing' and their dependence on the intercalate sublattice dimension. In the case of ESR studies, we also carried out a detailed analysis of dependence of the shape of the resonance line of the GIC on geometrical sizes of the sample.

## Experimental

Synthesis of GIC $C_{5n}HNO_3$ ($n=2$, 4) for ESR studies was carried out on HOPG plates with different width ($l$), height ($h$) and thickness ($d$), where $l\times h$ is the square of a side of a sample perpendicular to the ***c***-axis. Two series of samples were synthesized for the two compounds with $n=2$ and $n=4$. In the first series for $n=2$ (4), $l$ changed in the interval 0.05–0.225 (0.04–0.22) cm at constant $h=0.5$ (0.5) cm and $d=0.01$ (0.018) cm. In the other series $d$ changed for $n=2$ (4) in the interval 0.1–0.34 (0.2–0.4) cm at constant $h=0.5$ (0.5) cm and $l=0.225$ (0.32) cm. Accuracy of the plates size determination was $\sim 5\times 10^{-3}$ cm.

Synthesis of compounds for ESCA was conducted on the plates with $d=0.05$ cm and $h\times l=0.9\times 0.9$ cm$^2$. Samples with $n=2$ and $n=4$ were synthesized in 'steaming' nitric acid with density $\rho=1.565$ g/cm$^3$ and in dilute nitric acid with $\rho=1.490$ g/cm$^3$, respectively. The GIC stage was controlled by the diffraction method. According to data of non-contact measurements of electroconductivity of $C_{10}HNO_3$ plates at 300 K, $\sigma_a\simeq 1.5\times 10^5$ ohm$^{-1}$ cm$^{-1}$. According to literature data for $C_{5n}HNO_3$ $\sigma_c(n=2)\simeq 2$ ohm$^{-1}$ cm$^{-1}$ and $\sigma_a(n=4)\simeq 3.2\times 10^5$ ohm$^{-1}$ cm$^{-1}$ [5].

ESR measurements in X (Q) band were conducted in the rectangular (cylindrical) resonator with mode $TE_{102}$ ($H_{011}$) at 2.5 (100) kHz modulation and at $T=100$–300 K. In the rectangular resonator, the structure of the electromagnetic field of the $TE_{102}$ mode has such a form that at a conventional setting of resonator a constant magnetic field ***H*** is parallel to the electrical component ***E*** of the microwave field (MWF). GIC plates were placed in the resonator in such a way that basic and two lateral sides ($h\times d$) were parallel to the magnetic component (***H***) of the MWF. In the area of $T_c$, temperature changed gradually with a step $\Delta T\simeq 0.2$ °C and was kept up with accuracy $\sim 0.1$ °C/h.

ESCA measurements of C(1s), N(1s) and O(1s) electron spectra of GIC $C_{10}HNO_3$ plates were made with application of Mg K$\alpha$ radiation in the interval 170–300 K with residual pressure in a chamber of an energy analyser at $\sim 5\times 10^{-8}$ Torr. Resolution for the $4f_{7/2}$ gold peak was 1.4 eV. Variations of binding energies of C(1s) and N(1s) electrons were determined relative to the energy of O(1s) electrons which was supposed to be constant. Accuracy of temperature maintenance in the ESCA experiments was $\sim 2$ °C/h.

## Results

The single ESR signal of $C_{10}HNO_3$ with axial angular dependence relative to the ***c***-axis and $g_{\parallel}=2.0023\pm 0.0002$ and $g_{\perp}=2.0028\pm 0.0002$ is observed in both GIC phases from all plates. At $T<T_c$, lineshapes have a 'normal'

phase – in the sense that peak $A$ is situated in smaller magnetic fields relative to peak $B$ and the $A/B(l)$ curve has one gentle sloping maximum at $l(\text{max.}) = 0.1$ cm (Fig. 1). At $T > T_c$, $A/B(l)$ dependence has a four-peaked shape. At $\theta = 90°$ ($\theta$ = angle between $\boldsymbol{c}$ and $\boldsymbol{H}$) the $A/B(l)$ maximum is observed at $l'(\text{max.}) = 0.105$, 0.125, 0.140 and 0.170 cm. Plates with $l'(\text{max.})$ have a symmetrical lineshape relative to peak $A$. For plates with $l$ from three adjoining areas between $l'(\text{max.})$, peak $A$ of the line is situated in larger magnetic fields in comparison with peak $B$ (a 'reversed' phase) (Fig. 1). The single ESR signal of $C_{20}HNO_3$ has the same direction of the axis and values of $\boldsymbol{g}$ tensor as the second-stage sample. For all studied sizes of samples and temperatures, the lineshapes have a 'normal' phase. At $T > T_c$ ($T < T_c$) the $A/B(l)$ curve has one gentle sloping maximum at $l(\text{max.}) = 0.12$ (0.09) cm. In both stages of the GIC at $l \to 0$, the lineshapes tend to Lorenzian, independent of temperature. At constant $l$ and $h$, $A/B$ and 'phase' of the lineshapes do not depend on $d$.

On the basis of the $A/B(l)$ dependence of $C_{10}HNO_3$ ESR lines (Fig. 1(a)) for temperature studies in X band, we selected plates with $l' = 0.18$ cm for which $A/B$ variation at the phase transition is close to maximum and samples with $l > 0.22$ cm and corresponding $A/B$ values from the 'plateau' of $A/B(l)$ curves. Temperature studies of the $C_{10}HNO_3$ ESR signal were performed on plates having $l = 0.1$ cm. The regime of passage of phase transition was chosen based on the studies of temperature dependence of time $\Delta\tau(T)$ from the moment of gradual variation of temperature on $\Delta T$ to saturation of peak intensity of the ESR signal. On cooling (heating) the second-stage samples at $T_c^-$ ($T_c^+$) $= 250 \pm 0.5$ ($253 \pm 0.5$) K, the dependence $\Delta\tau(T)$ has a clear maximum. This temperature was taken as the phase transition temperature in $C_{10}HNO_3$ later on.

At $T > T_c$, the width ($\Delta H$), the integral intensity $I = (A + B)\Delta H^2$ and the $A/B$ of ESR lines for $n = 2$ and 4 do not depend on temperature. For $n = 2$ at $T_c$, all parameters of the line undergo sharp, nearly step-wise changes (Fig. 2). In the crystal phase of the intercalate, $\Delta H$ ($I$) increases (decreases) as temperature decreases. Simultaneously, the $A/B$ value of the samples, with $l'$ ($l > 0.22$ cm) for $n = 2$, decreases to $\sim 3.4 \pm 0.1$ ($3.0 \pm 0.2$) at saturation obtained at $T \sim 100$ K. Curve $\Delta H(T)$ for $n = 2$ in the interval $(T_c - 10) < T < T_c$ has a peculiarity: it consists of several linear sections with different slopes. One of them observed at $(T_c - 2.7) < T < (T_c - 1.9)$ K is parallel to the abscissa axis. It is interesting to note that the curve for $n = 4$ also contains the parallel section corresponding to the abscissa axis, which is situated between two inclined parts (Fig. 3). Integral intensities of signals also do not change in this interval of temperature. At temperature increase, parameter values of the ESR line change in a reverse consequence, but with a 'global' temperature hysteresis (Figs. 2 and 3). Transitions between corresponding linear sections of the $\Delta H(T)$ curve of the present sample take place for both stages at the same parameter values of the line, independent of direction of temperature variation. At powers of MWF far from saturation and at the same $T$, $\Delta H$ values in Q band are $\sim 15\%$ more than that in X band.

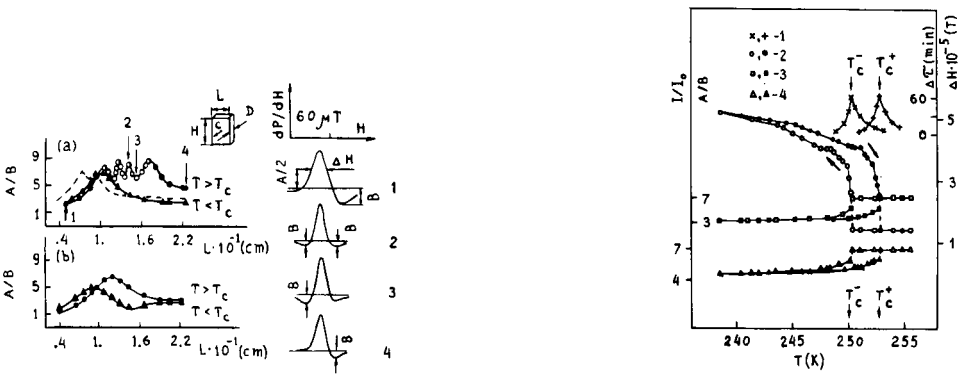


Fig. 1. $A/B$ parameter of the ESR first-derivative absorption line $A/B$ of $C_{10}HNO_3$ (a) and $C_{20}HNO_3$ (b) at $c \perp H$ for $T > T_c$ and $T < T_c$ on width ($l$) of the plates. In (a), $A/B(l)$ dependence of the ESR line of HOPG conduction electrons (dashed line) is shown for comparison. GIC plate dimensional parameters are shown in the upper part. ESR signals of the second-stage GIC for $l$ values marked by pointers are also shown. Lineshapes of type 2, 3 and 1 or 4 correspond to half-dark, light and dark points, respectively: (a) $d = 0.01$ cm, $h = 0.5$ cm; (b) $d = 0.018$ cm, $h = 0.5$ cm, $f = 9.52$ GHz.

Fig. 2. Dependence of $\Delta\tau$ (curve 1) and parameters of the ESR line of $C_{10}HNO_3$, i.e., $\Delta H$ (curve 2), $A/B$ (curve 3) and $I/I_0$ (curve 4), where $I_0$ = intensity of a standard signal, on temperature at crystallization (melting) of the intercalate. Unfilled (filled) symbols correspond to experimental values of parameters at cooling (heating) of the GIC: $d = 0.01$ cm, $h = 0.5$ cm, $l = 0.18$ cm, $f = 9.52$ GHz.

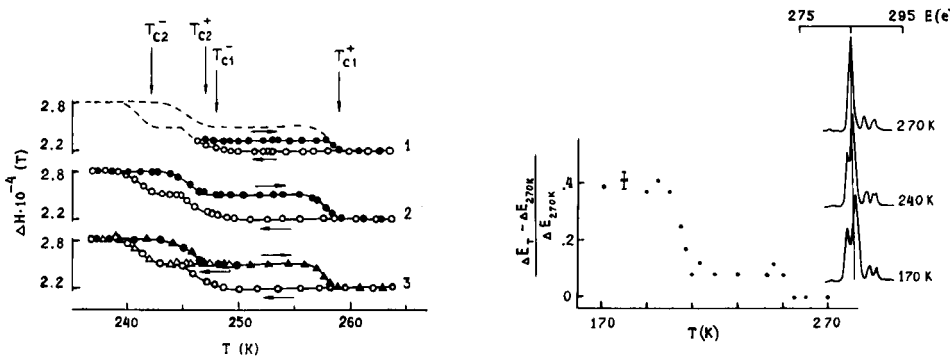


Fig. 3. Temperature dependence of ESR linewidth $\Delta H$ of $C_{20}HNO_3$ at crystallization (melting) of intercalate. Unfilled (filled) symbols correspond to experimental values of parameters at cooling (heating) of the GIC. Curves 1, 2 and 3 correspond to different limiting values of temperature passing from liquid to solid phases of the intercalate.

Fig. 4. Temperature dependence of lineshape and relative increase of full-width at half-maximum $(\Delta E_T - \Delta E_{270})/\Delta E_{270}$ of the ESCA spectrum of C(1s) electrons of GIC $C_{10}HNO_3$.

At $T > T_c$, binding energies (full-widths at half-maximum = $\Delta E$) of one-peak lines of core C(1s), O(1s) and N(1s) electrons of $C_{10}HNO_3$ do not depend on temperature. They are $285.0 \pm 0.1$ ($2.4 \pm 0.1$), $533.0 \pm 0.1$

$(2.6 \pm 0.1)$ and $407.3 \pm 0.1$ $(2.2 \pm 0.1)$ eV, respectively. At $T_c$, all lines widen unevenly and the spectrum of C(1s) electrons has a shape with two peaks. These peaks of the C(1s) spectrum are situated on different sides of the corresponding carbon line observed at $T > T_c$. The $\Delta E(T)$ curve of C(1s) electrons has two gentle sloping sections (Fig. 4). A smooth transition between these parts takes place at such temperatures when restricted rotations of $HNO_3$ molecules [6] are 'frozen' ('refrozen') on cooling (heating) a compound studied. It is interesting to note that in the same temperature interval, the two-step temperature dependence of the $C_5HNO_3$ ESR linewidth was discovered [7, 8]. The width of the N(1s) electron line increases as the temperature decreases and at $T < 200$ K is equal to $\Delta E = 2.8 \pm 0.2$ eV. At $T < T_c$, $\Delta E$ of O(1s) electrons does not depend on temperature and is equal to $3.0 \pm 0.1$ eV. All described variations of spectra are reversible in temperature within the limits of experimental accuracy.

## Discussion

The multipeaked shape of the $A/B(l)$ curve with areas of 'reversed' phase of the lineshape with $A/B > 2.55$ at large $l$ (on the plateau) testifies high mobility of spin carriers in $C_{10}HNO_3$ at $T > T_c$ [9] and, vice versa, the single-peaked $A/B(l)$ dependence, with $A/B \simeq 3$ at large $l$, is typical for weak diffusion spins in metals [9]. Consequently, the mobility of spin carriers at the phase transition in $C_{20}HNO_3$ in ESR time scale decreases and only weak diffusion spins are present in the intercalate crystal phase. From the above discussion and Fig. 3, it can be concluded that in both phases of the fourth-stage GIC only weak diffusion spins are present. The independence of $\boldsymbol{g}$ tensor values of spin carriers at changes of aggregate states of the intercalate and their closeness to the $g$ factor of the free electrons testify that the density of their probability on intercalate molecules is small and does not change at phase transition. A very weak frequency dependence of $\Delta H$ indicates that its growth at lower $T_c$ is not due to increase of degree of axis scattering and (or) values of $\boldsymbol{g}$ tensor. Comparison of Figs. 2 and 3 indicates that the values and character of variations of $\Delta H$ curves essentially depend on stage index, i.e., on the dimension of intercalate sublattice. However, it is of interest that at intercalate crystallization the full values of $\Delta H$ increasing are the same in both stages. By assuming that the centres of perturbation of conduction electron spin wave functions are situated preferentially at the edges of the Dumas–Herold islands [10], the mentioned independence of $\Delta H$ value increasing at $T$ on GIC stage index and the observation of larger values of $\Delta H$ for compounds with larger stage index can be put down to increasing the number and decreasing the size of Dumas–Herold islands in GICs with large stage index. In particular, charged ions $NO_3^-$ and paramagnetic radicals $NO_2$ can serve as perturbation centres.

The observed variations of lineshapes of core electrons in the $C_{10}HNO_3$ incommensurate phase can be explained by the presence of CDWs in surface

layers of GIC. In fact, inhomogeneous distributions of intercalate molecules, a kind of one-dimensional lattice of striped domains, is realized in $C_{10}HNO_3$ at lower $T_c$ [2]. The acceptor GIC intercalate layer contains both neutral molecules and negatively charged fragments [1, 11]. Therefore, its crystallization and the formation of the mass density wave may lead to modulation of concentration of negative charge in a layer. Exciting influence of this layer on the $\pi$-electronic graphite subsystem may initiate instability, a kind of CDW with a wave vector parallel to carbon planes through the electron–phonon interaction. According to ref. 12, the CDW presence leads to the appearance of additional energetic correction for formation of a 'hole' in its core shells. It leads to widening of X-ray photoelectronic lines of core-shell electrons of several atoms with transformation of their forms up to a two-peaked shape at increase of CDW amplitude. At $T<T_c$, conductivity of $C_{10}HNO_3$ plates increases $\sim$20% [11]. This indicates formation in this GIC at $T<T_c$ of CDWs localized only in its surface layers.

## References


1 M. S. Dresselhaus and G. Dresselhaus, *Adv. Phys., 30* (1981) 139–326.
2 H. J. Samuelseen, R. Moret, H. Fuzellier, M. Klatt, M. Lelaurain and A. Hérold, *Phys. Rev. B, 32* (1985) 417–427.
3 R. Clark, P. Hernandez, H. Homma and E. Montague, *Synth. Met., 12* (1985) 27–32.
4 M. J. Bottomley, G. S. Parry and A. R. Ubbelohde, *Proc. Roy. Soc. London, Ser. A, 297* (1964) 291–302.
5 A. R. Ubbelohde, *Proc. Roy. Soc. London, Ser. A, 231* (1972) 445–454.
6 F. Battalan, I. Rosnman, A. Magerl and H. Fuzellier, *Phys. Rev. B, 32* (1985) 4810–4813.
7 P. Lauginie, J. Conard, H. Estrade, D. Guérard, M. El Makhini, P. Lagrange, H. Fuzellier, G. Furdin and R. Vasse, *14th Biennial Conf. Carbon. Ext. Abstr., Pennsylvania State University, 1979*, pp. 312–313.
8 P. Lauginie, unpublished data.
9 H. J. Kodera, *Phys. Soc. Jpn., 28* (1970) 89–98.
10 N. Dumas and A. Hérold, *C. R. Seances Acad. Sci., Ser. C, 268* (1969) 373.
11 S. A. Solin, *Adv. Chem. Phys., 49* (1982) 455–532.
12 M. F. Bishop, S. M. Bose, P. Longe and S. Prutzer, *Phys. Rev. B, 36* (1987) 9341–9344.